UC Riverside
UC Riverside Previously Published Works

Title

Mechano-Responsive Piezoelectric Nanofiber as an On-Demand Drug Delivery Vehicle

Permalink

https://escholarship.org/uc/item/7vv8q79w

Journal

ACS Applied Bio Materials, 4(4)

ISSN

2576-6422

Authors

Jariwala, Tanvi
Ico, Gerardo
Tai, Youyi
et al.

Publication Date

2021-04-19

DOI

10.1021/acsabm.1c00232

Peer reviewed

Mechano-responsive piezoelectric nanofiber as an

on-demand drug delivery vehicle

Tanvi Jariwala[1‡], Gerardo Ico[1‡], Youyi Tai[1], Honghyun Park[2], Nosang V. Myung[3], and Jin Nam[1]*

[1]Department of Bioengineering, University of California, Riverside, Riverside, CA 92521, USA

[2]Korea Institute of Materials Science, 797 Changwondaero, Seongsan gu, Changwon, Gyeongnam, South Korea

[3]Department of Chemical and Biomolecular Engineering, University of Notre Dame, Notre Dame, IN 46556, USA

‡: equally contributed

*: corresponding author

Jin Nam, Ph.D., Department of Bioengineering, University of California, Riverside, Riverside, CA 92521, E-mail: jnam@engr.ucr.edu, Tel: 951-827-2064

Keywords: piezoelectric, electrospun fibers, on-demand drug delivery, mechano-sensitive

Abstract

The control over biodistribution and pharmacokinetics is critical to enhance the efficacy and minimize the side effects of therapeutic agents. To address the need for an on-demand drug delivery system for precise control over the release time and the quantity of drugs, we exploited the mechano-responsiveness of piezoelectric poly(vinylidene fluoride-trifluroethylene) (P(VDF-TrFE)) nanofibers for drug delivery applications. The large-surface-area-to-volume ratio inherent to nanomaterials, together with the transformative piezoelectric properties, allowed us to use the material as an ultrasensitive and mechano-responsive drug delivery platform driven by the direct piezoelectric effect. The intrinsic negative zeta potential of the nanofibers was utilized to electrostatically load cationic drug molecules, where surface potential changes by exogenous mechanical actuation trigger the release of drug molecules. We show that the drug release kinetics of the P(VDF-TrFE) nanofibers depends on the fiber diameter, thus piezoelectric properties. We further demonstrated that the drug release quantity can be tuned by the applied pressure or dose of physiologically safe corporeal shockwaves as a mechanical stimulus in *in vitro* and *ex vivo* models. Overall, we demonstrated the novel utility of piezoelectric electrospun nanofibers for mechano-responsive controlled drug release.

1. Introduction

Systemic drug administration is common for the treatments of chronic diseases, either through oral administration or with an injection of drugs. Despite the effectiveness and simplicity of these treatments, they require repeated administration to maintain a therapeutic level of the drug in the body, posing several challenges. The alternation of drug levels from high peaks at administration times to sub-therapeutic levels due to the first-pass metabolism of the drug requires initial overdosing to maintain the drug concentrations above therapeutic levels over a duration[1]. This deems conventional drug delivery an inefficient approach for chronic diseases, which require a sustained treatment with optimal dose and duration.

Several different approaches have been investigated to develop effective drug carriers in overcoming these limitations and improving the efficacy of therapeutic agents. Encapsulation or conjugation of drug molecules in a protective carrier, for example, prevents degradation and improves pharmacokinetic and pharmacodynamic properties, resulting in better controllability of its delivery[2]. Nanoparticles are attractive for such drug carriers due to their high surface-to-volume ratio, enhancing their drug loading capacity[3]. Biodegradable polymers in the form of nanoparticles are often used to enhance the biocompatibility of the carriers, but their passive release nature remains a disadvantage for temporally dynamic drug delivery[4].

Stimuli-responsive drug delivery systems are promising methods to overcome the limitation of the passive drug delivery systems by utilizing functional nanomaterial capable of releasing their drug payloads in response to physiological or externally applied triggers. For example, diseases that shift the physiological conditions such as pH, presence of reactive oxygen species, or inflammation trigger the drug carrier to release surface decorated drugs or bodily encapsulated drugs[5-7]. Similarly, externally controlled stimuli such as thermo-responsive release, light-responsive release, ultrasound-responsive release, and magnetic-responsive release are other

avenues to circumvent the limitations associated with degradation-based release[8-13]. Among these stimuli-responsive drug delivery systems, the electrically activated release of adsorbed molecules from the surface of electroactive materials is yet another method for controlled drug release schemes. For example, graphene oxide nanocomposite films can adsorb anionic drug molecules and release them on demand with an externally applied negative potential[14]. One of the major advantages of such a release scheme is its capability for fine-tuning the release kinetics by the magnitude of applied potential. However, it requires an external power source, diminishing enthusiasm for its internal use in the body.

In this regard, piezoelectric materials may provide a superior platform for the electrically controlled drug delivery system, due to their ability in converting mechanical forces to electric potentials through the direct piezoelectric effect. When piezoelectric materials are subjected to a dynamic strain, they rearrange dipole moments and develop an electric potential across their surfaces, thus bypassing the need for external electrical connections. Many inorganic materials including lead zirconate titanate (PZT), zinc oxide (ZnO), barium titanate (BaTiO3), possess high piezoelectric performance, requiring low magnitudes of mechanical perturbation for their activation[15, 16]. However, they present cytotoxicity[17] and/or instability in aqueous conditions[18], making them unfavorable for *in vivo* drug delivery applications. In contrast, polyvinylidene fluoride (PVDF) and its derivatives, organic materials capable of exhibiting piezoelectricity when optimally processed[19], have excellent biocompatibility that is currently being used as a vascular suture[20]. The mechanically soft nature of the polymer also reduces the formation of fibrous tissues encapsulating the implants and impacting drug release kinetics, often associated with hard materials[21]. The native negative surface charge of PVDF readily induces the adsorption of cationic molecules and also presents opportunities for facile surface modification according to the

characteristics of target drug molecules. However, it intrinsically exhibits inferior piezoelectricity as compared to the inorganic piezo-materials[18], requiring very high magnitudes of mechanical forces to piezoelectrically activate the material, diminishing its value for an *in vivo* drug delivery platform. In this regard, we have recently shown a transformative enhancement of piezoelectric polyvinylidene-trifluoroethylene (P(VDF-TrFE)) via nanoscale dimensional reduction and thermal treatment of the synthesized nanofibers[22]. This significantly increased piezoelectric coefficient (108 pm V^{-1}) in P(VDF-TrFE), comparable to those in typical inorganic piezoelectric materials, allows for developing a wide range of electromechanically sensitive flexible devices.

In this work, we have developed a mechanical stimulus-responsive or mechano-responsive drug delivery system, based on piezoelectric nanofibers, and demonstrated its capability for controlled drug release *in vitro* and *ex vivo*. We showed that the drug release characteristics of P(VDF-TrFE) nanofibers can be fine-tuned by modulating their piezoelectric properties via fiber size control, thus the sensitivity of the material to the magnitude and frequency of the applied forces. Different model drugs were utilized to demonstrate that drug release kinetics is fully governed by the mechano-electrical conversion from the physiologically safe-magnitudes of applied mechanical perturbation to change surface potentials, regulating the adsorption/release of electrostatically adhered drug molecules. A 3D hydrogel *in vitro* study, as well as an *ex vivo* study using porcine skins, was performed to show the controllability of drug release in a 3D construct resembling the physiological environments, demonstrating the promising potential of piezoelectric nanofibers for controlled drug delivery.

2. Materials and Methods

2.1. Electrospinning of P(VDF-TrFE) nanofibrous membranes

Nanofibrous membranes composed of approximately 30 nm in diameter P(VDF-TrFE) nanofibers were synthesized by preparing a solution containing 4.0 wt.% P(VDF-TrFE) (70/30 mol%) (Solvay Group, France) dissolved in a 50/50 weight ratio of N,N-dimethylformamide (DMF) (Fisher Scientific, Pittsburgh, PA), and tetrahydrofuran (THF) (Sigma-Aldrich, St. Louis, MO). The solution was supplemented with 1.5 wt.% pyridinium formate (PF) buffer (Sigma-Aldrich) and 0.05 wt.% BYK-377 (BYK Additives and Instruments, Wesel Germany) to increase the solution conductivity and decrease the surface tension, respectively. Nanofibers with an average fiber diameter of approximately 70, 100, 200, or 500 nm fibers were separately synthesized from a solution of 6.0, 7.0, 11.5, and 17.5 wt.% P(VDF-TrFE), respectively, dissolved in a 60/40 ratio of DMF/acetone(Fisher Scientific, Pittsburgh, PA), and 1.5 wt.% PF buffer. As a control, a solution of 13.5 wt.% of PVDF dissolved in the same DMF/acetone/PF solvent system was prepared to synthesize fibers of approximately 500 nm. Each solution was electrospun under optimized conditions of electrospinning distance (20 cm), applied voltage (approximately -15 kV) and solution feed rate (0.2 mL hr^{-1} for the 4.0, 6.0 and 7.0 wt.% solutions; 0.5 mL hr^{-1} for the 11.5 and 17.5 wt.% solutions) at 23 °C with an absolute humidity of approximately 7.6 g m^{-3}. Electrospinning duration was adjusted to yield approximately 20 μm thick mats on a 76 x 76 mm^2 aluminum foil collector. The P(VDF-TrFE) nanofibrous membranes were subsequently annealed at 90 °C for 24 hrs to further improve their piezoelectricity[22]. The control PVDF fibers, herein called heat-inactivated PVDF, were heat-treated in a rapid thermal annealing oven (Allwin21 Corp) for precise temperature control at 157 °C for 1 hr, followed by quenching in -20 °C ethanol, to induce the β- to α-phase transition for the suppression of piezoelectricity without any morphological changes[23].

2.2. Morphological and piezoelectric characterization of P(VDF-TrFE) and heat-inactivated PVDF nanofibers

The morphology of the electrospun fibers was characterized using a VEGA3 scanning electron microscope (SEM) (Tescan Brno, Czech Republic). The average fiber diameter (n=60) was measured using ImageJ software.

To properly measure the piezoelectric coefficient, d_{33}, a standard periodically poled lithium niobate (PPLN) with a known piezoelectric coefficient was used to determine a correction factor for all subsequent measurements. Various P(VDF-TrFE) or PVDF nanofibers were sparsely collected on a gold-coated, thermal-oxide silicon substrate, heat-treated, and subjected to single-point piezoresponse force microscopy (PFM) on individual fibers. An MFP-3D AFM (Asylum Research, Santa Barbara, CA) was first used in tapping imaging mode to locate an individual fiber. Five points were chosen on the scanned fiber and the AFM was switched to PFM mode where single point piezoresponse measurements were conducted. Step voltages from -3 to +3 V were applied across the fiber via the AFM cantilever (AC240TM, Olympus) to the grounded substrate. A value of d33 was calculated by,

$$d_{33} = \frac{A}{VQ}f$$
,

where A is the amplitude response of the nanofiber in response to an applied voltage (V), Q is the quality factor of the AFM cantilever, and f is the correctional factor taken from the PPLN standard. To quantify the electric potential generated on the surface of the P(VDF-TrFE) and heat-inactivated PVDF nanofibrous membranes, the membranes with dimensions of 1x1 cm^2 were subjected to the shockwave mechanical stimulation. These nanofibrous membranes having a gold-sputtered side as an electrode were placed in between two layers of nitrocellulose film (Bio-Rad, Hercules, CA) and pre-wetted with PBS. This construct was then placed in between two layers of

0.5 cm-thick PDMS slabs. A shockwave system (MP-100 Vet, Storz Medical, Tägerwilen, Switzerland) was used to deliver mechanical actuation with a pressure of 5 bar and a frequency of 12 Hz. The generated voltage on the surface of the nanofibrous membrane was simultaneously measured by an oscilloscope (Pico Technologies, UK) during the shockwave application.

2.3. Zeta potential measurements of nanofibrous membranes

The zeta potential of nanofibrous membranes was determined by measuring the streaming current formed tangentially to the fibrous surface with an electrokinetic analyzer (SurPASS Electrokinetic Analyzer, Anton Paar, Graz Austria). By utilizing the streaming current, the zeta potential (ζ) was calculated by,

$$\zeta = \frac{dI}{dP} \frac{\eta}{\varepsilon\varepsilon_0} \frac{L}{A},$$

where I is the measured streaming current, P the pressure difference across the length of the sample, η and ε the viscosity and dielectric constant of the electrolyte solution, ε_0 the dielectric constant of free space, L the channel length of the measured sample, and A the cross-sectional area along with the sample. Two- 1 cm x 2 cm cuts of each sample were fixed inside an adjustable gap cell of the electrokinetic analyzer and the gap between the two opposing faces of the sample was adjusted to approximately 100 μm. An electrolyte solution of 1 mM KCl was used to generate a titration curve of the zeta potential for each sample. The streaming current was logged after 20 seconds of flow-through of a given titration at a pressure of 400 mbar.

2.4. Drug loading onto nanofibrous membranes

In order to adsorb cationic model drug molecules on the surface of natively charged, hydrophobic PVDF derivatives, a 30-second pre-wash in ethanol was conducted on each sample to promote wettability of the P(VDF-TrFE) and heat-inactivated PVDF nanofibrous membranes. The ethanol treatment was followed by three washes with 1x PBS, prior to the subsequent drug loading in an aqueous condition. Crystal violet, a cationic model drug whose molecular structure and UV-vis spectral property were shown in **Figure S1**, was dissolved in PBS at 0.75 mg mL^{-1} for its adsorption onto a 1x1 cm^2 sample. After exposing the samples to the crystal violet solution overnight on a shaker plate, any loosely bound dye was removed from the nanofibrous membranes by a two-step washing process. The first step involves a diffusion-based desorption method in fresh PBS for 24 hrs on a shaker plate, followed by the second step where the sample was further washed with PBS through a vacuumed filter. After this washing process, any spontaneous leakage was not detected under a static incubation in PBS for 1 week. To determine the drug loading capacity of crystal violet onto P(VDF-TrFE) nanofibrous membranes with 30 and 500 nm fiber diameters, following equations were used.

$$C_f = \frac{C_i \cdot A_f}{A_i} \qquad\qquad q = \frac{(C_i - C_f)V}{W}$$

where C_i is the initial dye solution concentration, C_f is the final dye solution concentration, A_f is the absorbance of the final dye solution, A_i is the absorbance of the initial dye solution, V is the volume of dye solution, W is the mass of P(VDF-TrFE) nanofibrous membrane. The maximum amount of crystal violet loading on P(VDF-TrFE) nanofibrous membrane with 30 nm diameter and on heat-inactivated PVDF nanofibrous membrane with 500 nm diameter were 1850 μg and 750 μg per nanofibrous membrane (approximately 5 mg), respectively.

Poly(l-lysine) (PLL), another cationic model drug (**Figure S1**), was conjugated with a photoluminescence fluorochrome for *ex vivo* drug release experiments. Briefly, poly(l-lysine) hydrobromide (30-70 kDa, Sigma) was dissolved in 50 mM sodium borate buffer (Fisher Scientific) at pH 8.5. Vivotag-645 fluorochrome (PerkinElmer, Waltham, MA) (spectral property shown in **Figure S1**)**,** was added into the mixture for the final concentration of PLL and Vivotag-645 at 20 μM and 48 μM, respectively. The reaction was allowed to proceed under stirring for 6 hrs at room temperature. Vivotag-645-conjugated PLL was separately loaded onto 0.5x0.5 cm^2-sized P(VDF-TrFE) and heat-inactivated PVDF nanofibrous membranes in a similar manner as described in the crystal violet loading. The drug loading capacity of PLL/Vivotag-645 was determined to be 60 μg and 41.6 μg per 1 mg of 30 nm P(VDF-TrFE) and 500 nm heat-inactivated PVDF nanofibrous membranes, respectively.

2.5. In vitro drug release

All P(VDF-TrFE) and heat-inactivated PVDF nanofibrous membranes with a sample size of 1x1 cm^2 were loaded with the same amount of crystal violet (750 μg), placed between two layers of nitrocellulose film that acts as a drug-capturing film, and pre-wetted with PBS. This construct was placed between two layers of 0.5 cm thick PDMS slabs acting as buffer pads under the applied mechanical perturbation. A shockwave system was used to deliver the mechanical stimulation to the samples to induce the piezoelectric effect. The number of delivered shockwaves, as well as the applied pressure, was varied while maintaining the frequency fixed at 12 Hz. After each regimen, the nitrocellulose films, stained with crystal violet that was released by the drug-loaded nanofibrous membranes, were collected to be optically scanned for quantification. To test repeated on-demand drug releases, the crystal violet-loaded P(VDF-TrFE) samples, sandwiched in between

two nitrocellulose drug-capturing films, were subjected to shockwave applications at 5 bar, 12 Hz

for 5 mins every 2 hrs. The nitrocellulose films were collected immediately after the shockwave

applications as well as 10 mins before and after the applications to determine spontaneous drug

release. Briefly, optical density was measured using an image scanner at a resolution of 3200 dpi

from each nitrocellulose film and processed in ImageJ for total gray value quantification. The

images were converted to 32-bit, gray values inverted. The stain regions were manually selected

and analyzed for total gray value by multiplying the average gray value with the total pixel density

of the selected area. The standard curve shown in **Figure S2** was used to quantify the amount of

drug release.

  In order to determine drug release in 3D, simulating the conditions in soft tissues, drug-loaded

nanofibrous membranes were individually encapsulated within a hydrogel plug and subjected to

mechanical stimulation via shockwave applications. Two 0.5 cm thick and one 0.7 cm thick PDMS

slabs were synthesized to fit in a well of a 6-well plate. A hole, which will act as a hydrogel pocket,

was created in the middle of the 0.7 cm thick PDMS slab with a 6 mm biopsy punch. One of the

0.5 cm thick PDMS was placed at the bottom of the well and the 0.7 cm thick PDMS with the

pocket was placed on top of it. Half of the pocket was filled with gelatin methacrylate (GelMA),

synthesized as described elsewhere[24], photo-crosslinked by UV application. Then, a 0.5x0.5 cm^2

sample of P(VDF-TrFE) nanofibrous membrane, loaded with crystal violet, was placed on top of

the cured hydrogel and the other half of the pocket was filled with GelMA polymer solution and

photo-crosslinked to encapsulate the P(VDF-TrFE) nanofibrous membrane between two layers of

the hydrogel. The hydrogel pocket was sealed with another 0.5 cm thick PDMS slab. The

shockwave system as described previously was used to deliver mechanical stimulation to the

hydrogel to induce the piezoelectric effect of the P(VDF-TrFE) nanofibrous membranes. The

duration of shockwave application was varied while maintaining the applied pressure fixed at 5 bar with its frequency at 12 Hz. After the stimulation, the hydrogel plus was removed from the PDMS slabs to examine the drug release spread throughout the hydrogel.

Each hydrogel plug, after removing the P(VDF-TrFE) nanofibrous membrane, was minced and added to 400 µL of collagenase-IV (enzyme activity – 265 U mg^{-1}) (Worthington Biochemical Co, Lakewood, NJ) with 20 U mL^{-1} in PBS. Hydrogel in collagenase-IV solution was digested in an incubator (37 °C) for 24 hrs before colorimetric reading at a wavelength of 590 nm with a microplate reader (SpectraMax Plus 384, Molecular Devices, San Jose, CA).

2.6. Ex vivo drug release

Each 0.5x0.5 cm^2 sample of P(VDF-TrFE) or heat-inactivated PVDF nanofibrous membrane was loaded with 52 µg of PLL conjugated with Vivotag-645 and placed between two layers of porcine skin without subcutaneous fat and pre-wetted with PBS. The samples were then mechanically actuated using the shockwave system to induce the piezoelectric effect for drug release. For the P(VDF-TrFE) nanofibrous membranes, the duration of the shockwave actuation, as well as applied pressure, was varied while maintaining the frequency fixed at 12 Hz. As a non-actuated control, the drug-loaded P(VDF-TrFE) sample was sandwiched between porcine skins for 10 mins without actuation. For non-piezoelectric control, drug-loaded, heat-inactivated PVDF nanofibrous membranes were subjected to shockwave applications for 10 mins at 5 bar and 12 Hz. Alternatively, the drug-loaded P(VDF-TrFE) membranes were subjected to a repeated, on-demand drug release test, where the membranes were incubated in between two layers of porcine skin prior to being subjected to shockwave applications at 3 bar, 12 Hz for 2 mins. The shockwave applications were performed every other day for a total duration of 6 days. The porcine skins were

collected prior to the shockwave applications to determine spontaneous drug release. The photoluminescence of the top and bottom porcine skins after drug release was visualized in a luminescence dark box with a PIXIS 1024B camera (filter: 690 ± 50 nm). WinView software was used to determine photoluminescence intensity emitted from the Vivotag-645, where the sum of intensity values from the top and bottom porcine skins were used for drug release quantification.

2.7. Statistical analysis

All experiments were conducted at a minimum in triplicate unless otherwise noted. Data are represented as mean ± standard deviation. Statistical analysis was conducted to determine significance by one-way analysis of variance (ANOVA) with Tukey's posthoc testing using SPSS software (v.19.0, IBM Corp., Armonk, NY). A value of $p < 0.05$ was regarded as statistically significant.

3. Results

The working principle of our proposed mechano-responsive piezoelectric drug delivery platform is based on the control over electrostatic binding strength between a charged molecule and the surface of the P(VDF-TrFE) having a particular zeta potential. Due to the piezoelectricity of P(VDF-TrFE), a mechanical perturbation can effectively change the magnitude and polarity of the surface potential from the static state value (**Figure 1a**) to a value opposite to the intrinsic polarity (**Figure 1b**). This change in the surface potential of the P(VDF-TrFE), from negative to positive, would induce the release of the electrostatically adhered drug molecules; the mechanical perturbation alters the microscopic domains of the crystalline electroactive phase causing a shift in polarity which results in a net charge change at the surface of the P(VDF-TrFE). Thus, we

hypothesize that this mechano-responsive piezoelectric material can serve as an on-demand drug delivery system, where its sensitivity can be tuned by controlling the piezoelectric properties to precisely regulate drug release kinetics under a particular magnitude of mechanical stimulation.
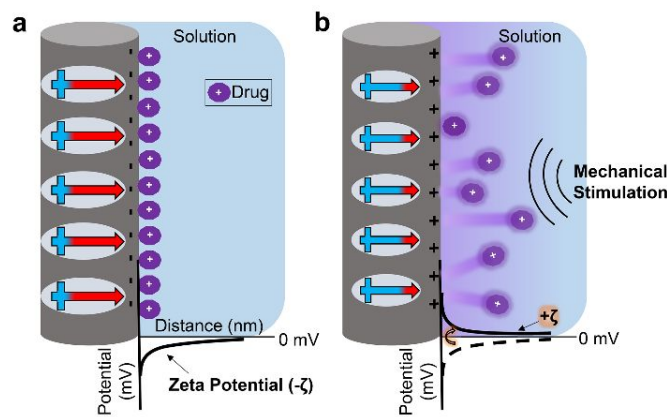

Figure 1. **Schematic of stimuli-responsive drug release.** (a) Piezoelectric dipole domains of P(VDF-TrFE) (blue to red arrows) at the static state with the associated negative zeta potential profile near the surface of an electrospun P(VDF-TrFE) nanofiber, inducing the attraction of cationic drug molecules. (b) Piezoelectric response of dipole domain change in polarity towards positive values under a mechanical perturbation, effectively overcoming the negative zeta potential, which subsequently repels the drug molecules away from the surface.

3.1. Piezoelectric and surface charge characterization of P(VDF-TrFE) and heat-inactivated PVDF nanofibrous membranes

To demonstrate the proof-of-concept of utilizing electrospun piezoelectric nanofibers as an on-demand drug delivery platform, several different variations of P(VDF-TrFE) nanofibers were synthesized and characterized. Similar to our previous study[22, 25], P(VDF-TrFE) nanofibers with different fiber diameters were synthesized by controlling electrospinning parameters such as solution concentration, conductivity, and surface tension (the P(VDF-TrFE) nanofibers with the average fiber diameters of 34 ± 18 nm (herein referred to 30 nm) and 476 ± 122 nm (herein referred

to 500 nm) are shown in **Figure 2a and 2b** as examples). In addition, heat-inactivated PVDF

nanofibrous membranes of 469 ± 144 nm (herein referred to 500 nm) in average fiber diameter

was synthesized and thermally treated between the Curie and melting temperature to eliminate the

piezoelectric phase but keep the fibrous morphology (**Figure 2c**). This heat-inactivated PVDF

sample was used as a control to determine whether the release of the model drug was mechanically

driven, piezoelectrically driven, or the combination of both. The piezoelectric performances of the

30 and 500 nm P(VDF-TrFE) nanofibers and the 500 nm heat-inactivated PVDF nanofibers were

determined from PFM measurements, showing their piezoelectric coefficient d_{33} at 103 ± 22, 37 ±

4, and 6 ± 2 pm V^{-1}, respectively (**Figure 2d**). However, the changes in piezoelectric properties

did not significantly alter the zeta potential, showing a similar value of approximately -50 mV at

the physiological pH range of 7.4 (the zeta potentials of 30, 500 nm P(VDF-TrFE), and 500 nm

heat-inactivated PVDF were approximately -48, -54, and -51 mV, respectively) (**Figure 2e**). Since

the zeta potentials across all samples are similar, therefore, the energy barrier that must be

overcome to release the drug can be considered similar for all samples tested herein. Electrical

potential generation of the 30 and 500 nm P(VDF-TrFE) nanofibers and the 500 nm heat-

inactivated PVDF nanofibers were peak-to-peak voltages of approximately 397, 41.6, and 7 mV,

respectively (**Figure 2f-h**). These results demonstrated that the electric potential generation of the

P(VDF-TrFE) nanofibrous membrane with 30 nm fiber diameter under shockwave application was

sufficiently greater than the zeta potentials, indicating that the electric potential is high enough to

inverse the polarity of the surface charge. Moreover, given the significantly low values of

piezoelectric coefficients and electrical potential generation, the heat-inactivated PVDF

nanofibrous membranes having 500 nm fiber diameter were used as a non-piezoelectric control to

examine the effect of mechanical perturbation in drug release for the rest of the study.
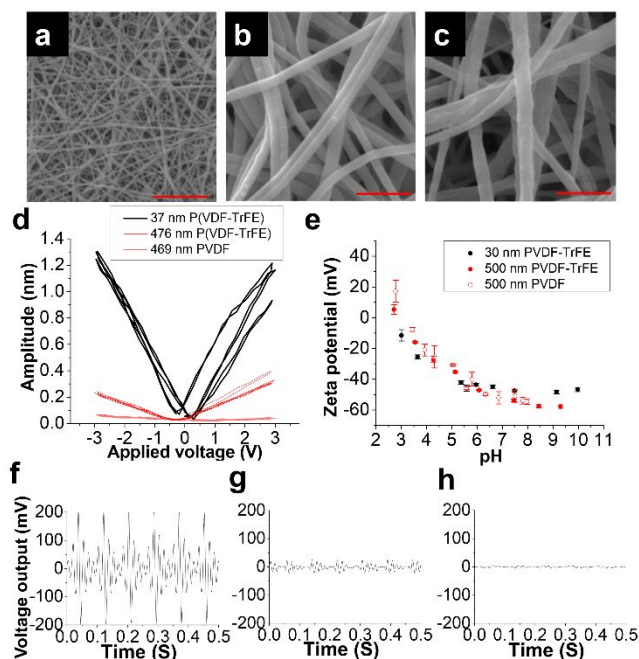
Figure 2. **Morphological, piezoelectric, and electrochemical characterization of various electrospun fibers.** SEM images of (a) 34 ± 18 and (b) 476 ± 122 nm piezoelectric P(VDF-TrFE) nanofibers, and (c) 469 ± 144 nm heat-inactivated PVDF nanofibers (scale bar = 2 μm). (d) Piezoresponse force microscopy of individual fibers from the three different samples (a-c) showing the decreasing piezoelectric performance of the P(VDF-TrFE) fibers by increasing fiber size, and virtually no piezoelectric response from the heat-inactivated PVDF fibers. (e) Zeta potential of the three samples showing similar values as a function of solution pH. Electric potential generation of (f) 30 nm P(VDF-TrFE) nanofibrous membrane, (g) 500 nm P(VDF-TrFE) nanofibrous membrane, and (h) 500 nm heat-inactivated PVDF nanofibrous membrane under shockwaves with a magnitude of 5 bar, and a frequency of 12 Hz.

3.2. Tunable drug release kinetics from P(VDF-TrFE) nanofibrous membranes via control over piezoelectric properties

To quantify the release of adsorbed drug molecules via the piezoelectric effect, crystal violet was used as a cationic model drug due to its simplistic nature of confirming adsorption by its color and quantifying release by colorimetry. In this regard, nitrocellulose film was used to act as a

molecule catcher upon the release of the drug in a solution for accurate detection at low concentrations. A titration study was conducted to generate a standard curve used to quantify the drug release from the piezoelectric nanofibers (**Figure S2**). The cationic model drug was loaded to various samples including P(VDF-TrFE) with different fiber diameters and heat-inactivated PVDF nanofibers, by incubating them in 1 mL aqueous solution of crystal violet at a concentration of 750 µg mL^{-1}, determined by the aforementioned measurement of crystal violet loading capacity. To test the release of adsorbed drug molecules in response to the mechanical stimulation, an extracorporeal shockwave system was utilized (**Figure 3a**). A 1x1 cm^2 nanofibrous membrane of each sample was loaded with the drug, pre-washed, and placed between two nitrocellulose films that catch released drug molecules. The assembly was then sandwiched between two pieces of PDMS to simulate soft tissues/muscles.

To show the fiber size-dependent, thus piezoelectric property-dependent effects of the drug release tunability, a study was conducted comparing the drug release from the aforementioned P(VDF-TrFE) nanofibrous membranes with an average fiber diameter of 30 or 500 nm, in addition to nanofibrous membranes with intermediate fiber sizes of 72 ± 14, 96 ± 15, and 210 ± 75 nm (herein referred to 70, 100, and 200 nm, respectively). All samples showed complete adsorption of the same concentration of drug in the solution (750 µg mL^{-1}) with no apparent change in the fiber morphology or fibrous structure (**Figure 3b-f**). Additionally, the heat-inactivated PVDF was also compared to show the maintenance of fibrous structure after the drug adsorption (**Figure 3g**). Furthermore, the apparent colors of the nanofibrous membranes of different fiber diameters after drug adsorption were indistinguishable (**Figure 3h**).
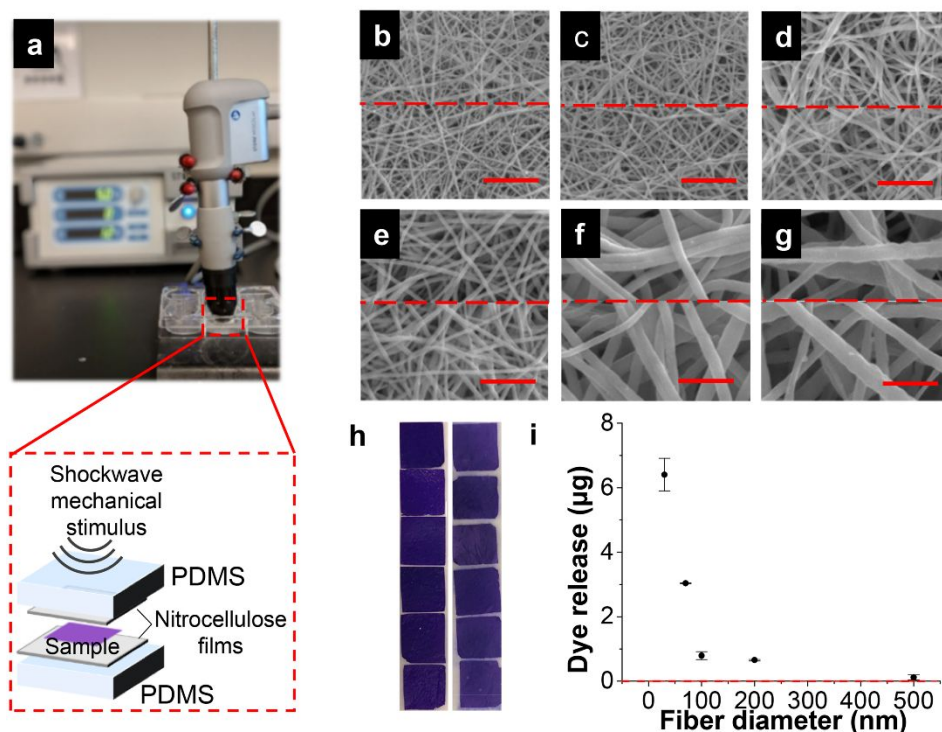
Figure 3. Piezoelectricity-dependent drug release. (a) An image and a schematic of an *in vitro* setup to simulate and quantify drug release under mechanical perturbation via shockwave applications. SEM images of (b-f) P(VDF-TrFE) and (g) PVDF nanofibrous membranes before (above red dashed line) and after (below red dashed line) adsorbing a model drug, crystal violet, having average fiber diameters of (b) 34 ± 18, (c) 72 ± 14, (d) 96 ± 15, (e) 210 ± 75, (f) 476 ± 122, and (g) 469 ± 144 nm (scale bar = 2 μm). (h) An optical image of drug-loaded membranes of (top to bottom) 34, 72, 96, 210, and 476 nm P(VDF-TrFE), and 469 nm PVDF membranes before (left column) and after (right column) 1000 shockwave doses at 5 bar/12 Hz. (i) Drug release amount after 1000 shockwave doses at 5 bar/12 Hz as a function of fiber diameter (n=5). The red dotted line indicates the amount of drug release from the heat-inactivated PVDF samples.

A dosage of 1000 shockwaves was delivered at a pressure of 5 bar and frequency of 12 Hz, to five replicates of each sample. The color intensity of the drug-loaded membranes after the shockwave application did not change significantly, likely due to relatively small release amounts of drug molecules as compared to the loaded amounts (**Figure 3h**). As expected from the greater

piezoelectric coefficients in smaller fiber sizes, the P(VDF-TrFE) nanofibrous membranes with smaller fibers released a greater amount of drugs under the shockwave application (**Figure 3i**). The effects of difference in surface area due to different nanofiber diameters can be disregarded since all samples were loaded with the same amount of the drug. Moreover, the heat-inactivated PVDF showed a negligible amount of drug release compared to all other samples such that the amount released from the 500 nm P(VDF-TrFE) sample was approximately 200-fold greater than that of the 500 nm heat-inactivated PVDF sample (red dashed line in **Figure 3i**).

To further demonstrate the utility of piezoelectric nanofibers as a mechano-responsive drug delivery system capable of releasing a controlled amount of molecules, the high-performing 30 nm fibers were tested as a function of the applied pressure and shockwave dosage, as shown in **Figure 4a** and **Figure 4b**, respectively. An increase in the amount of drug release is observed as the pressure of the shockwave system is increased from 1 to 5 bar. From 1 to 2.5 bar a relatively linear trend is observed, while from 3-5 bar an exponential trend is observed. Additionally, the amount of drug released with respect to the number of shockwaves (500, 1000, 2000, and 4000 applications at 5 bar and 12 Hz) shows a linear increase, indicating a controllable release of adsorbed molecules. On-demand release capability was tested by subjecting the drug-loaded P(VDF-TrFE) nanofibrous membranes to repeated shockwave applications with intervals (**Figure 4c**). A similar level of drug release was observed for each shockwave stimulation while no spontaneous drug release was observed during incubation between mechanical stimulations, confirming the specificity of drug release induced by mechanical piezoelectric activation without diffusional leaks.
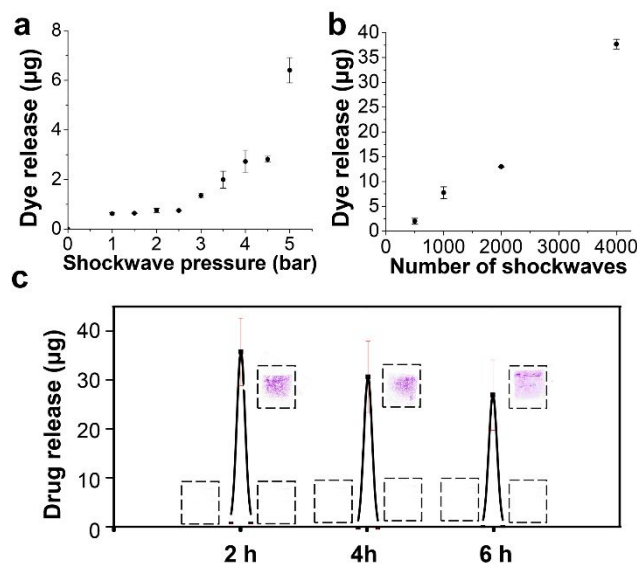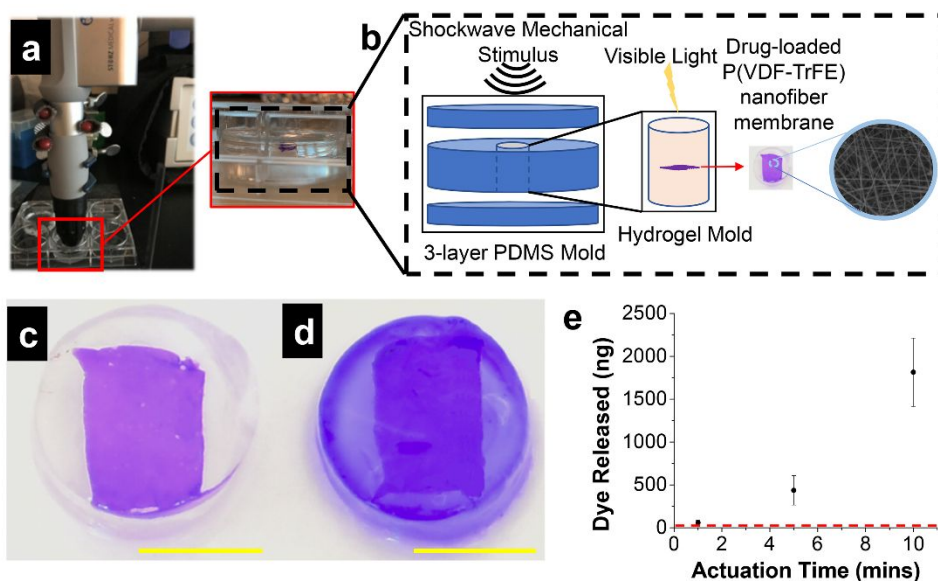
Figure 4. Mechano-responsive drug release. Drug release of P(VDF-TrFE) nanofibrous membranes having an average fiber diameter of 30 nm, loaded with a model drug, crystal violet, as a function of (a) shockwave pressure (at 1000 shockwaves/12 Hz) and (b) number of shockwaves (at 5 bar/12 Hz) (n=5). (c) On-demand drug release profile of crystal violet-loaded P(VDF-TrFE) nanofibrous membranes having an average fiber diameter of 30 nm, where the membranes were stimulated by shockwaves at 5 bar/12 Hz for 5 mins every 2 hrs (insets: optical images of drug-capturing nitrocellulose films).

3.3. Controlled drug release in 3D

The controlled drug release performance of piezoelectric nanofibrous membrane was also demonstrated in a 3D construct of a hydrogel, better resembling the 3D physiological environment. Similar to the 2D release onto nitrocellulose films as previously described, an extracorporeal shockwave system was utilized to provide mechanical perturbations to the drug-carrying P(VDF-TrFE) nanofibrous membrane encapsulated within hydrogel (**Figure 5a**). The hydrogel plug which encapsulated a 0.5x0.5 cm² P(VDF-TrFE) nanofibrous membrane loaded with the drug, was sandwiched between two pieces of PDMS with its elastic modulus approximately at 10 kPa, acting as soft tissues (**Figure 5b**).

To show the dose-dependent effect on the drug release tunability in a 3D environment, different durations of shockwave actuation were applied on the drug-loaded nanofibrous membrane/hydrogel constructs for 1, 5, or 10 mins at 5 bar and 12 Hz. Optical images of the hydrogel with the nanofibrous membrane before (**Figure 5c**) and after (**Figure 5d**) shockwave application clearly show the release of the drug as a response to the mechanical stimulation. Similar to the 2D condition, the piezoelectric nanofibrous membranes released a greater amount of drugs with increasing duration of mechanical stimulation, demonstrating the piezoelectric performance of the drug delivery vehicle in a 3D environment (**Figure 5e, Figure S3**).
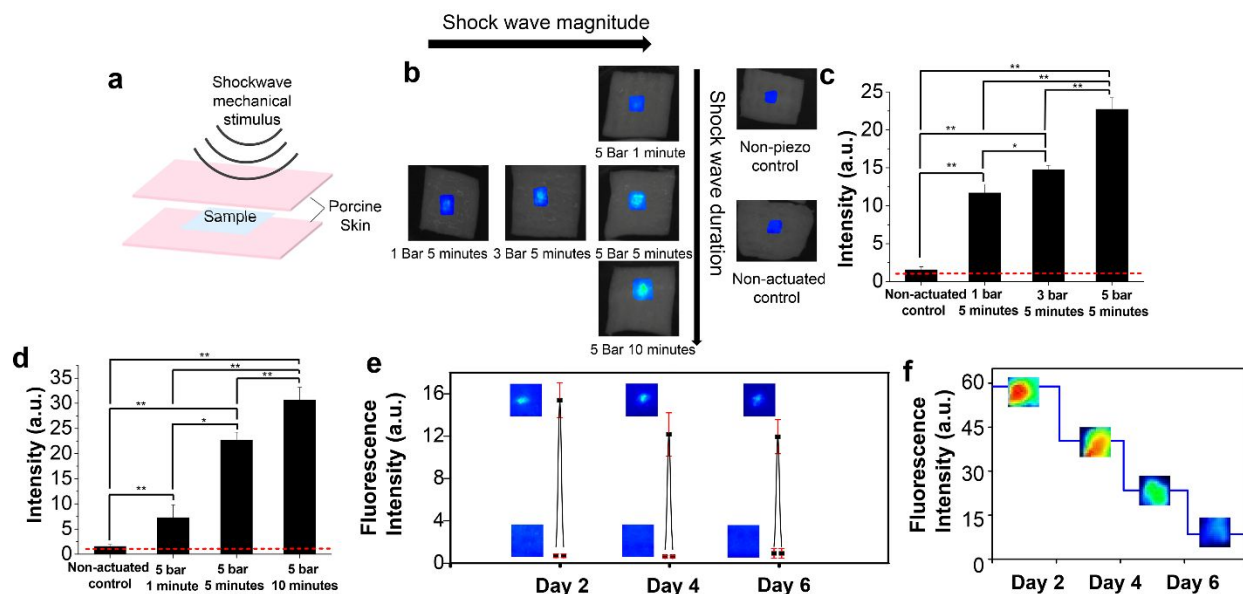

Figure 5. **Mechano-responsive drug release in 3D.** (a) An image of the shockwave system applying mechanical stimulation for *in vitro* drug release in 3D. (b) A schematic of the *in vitro* set up consisting of drug-loaded electrospun P(VDF-TrFE) nanofibrous membrane encapsulated within a hydrogel pocket in the middle of a PDMS mold and sealed with two layers of PDMS membranes. (c-d) Optical images of the hydrogel plug containing a drug-loaded electrospun P(VDF-TrFE) nanofibrous membrane (c) before and (d) after mechanical stimulation through shockwave application (Scale bar = 6 mm). (e) Quantification of drug release from crystal violet-loaded P(VDF-TrFE) nanofibrous membrane as a function of the duration of shockwave application (at 5 bar/12 Hz). The red dotted line indicates the drug release from heat-inactivated PVDF samples.

3.4. Controlled drug release ex vivo

An *ex vivo* porcine skin model was utilized to further demonstrate the feasibility of the mechano-responsive drug delivery system for controlled drug release. A 0.5x0.5 cm^2 sample of drug-loaded P(VDF-TrFE) nanofibrous membrane was placed between two pieces of porcine skin, with the dermis facing the nanofibrous membrane, and subjected to mechanical stimulation using the shockwave system at a physiologically-safe magnitude (**Figure 6a**). Two 3x3 cm^2 porcine skins without subcutaneous fat and pre-wetted with PBS were utilized. Photoluminescence images of the Vivotag-645 fluorophore from the porcine skins after actuation showed increased drug release amounts in response to an increase in shockwave pressure and duration (**Figure 6b**). A non-piezoelectric control, the heat-inactivated PVDF nanofibrous membrane actuated for 10 mins at 5 bar, and a non-actuated control, the P(VDF-TrFE) nanofibrous membrane without shockwave application, showed negligible drug release as compared to actuated P(VDF-TrFE) fibers, confirming that the drug release was induced by the piezoelectric effect. Quantification of photoluminescence images demonstrated that the drug release in soft tissues can be controlled by both the magnitude and duration of mechanical perturbation (**Figure 6c and d**). Similar to the results of crystal violet release, there was a minimal spontaneous release of the drug during the incubation in between the skins for 2 days while responding to repeated shockwave applications with a similar drug release amount in 2-day intervals (**Figure 6e and f**).

Figure 6. Mechano-responsive drug release *ex vivo*. (a) A schematic of an *ex vivo* setup to simulate and quantify drug release in soft tissues under mechanical perturbation via shockwave applications. (b) Photoluminescence images showing the intensity of a model drug (poly(l-lysine)-Vivotag-645) released onto the porcine skins after actuation of the drug-loaded P(VDF-TrFE) nanofibrous membranes with various applied shockwave pressures and durations. Photoluminescence images showing a minimal amount of model drug released onto the porcine skin for non-piezoelectric control (heat-inactivated PVDF nanofibrous membrane after actuation) or non-actuated control (P(VDF-TrFE) nanofibrous membrane without actuation). Photoluminescence intensity values from P(VDF-TrFE) nanofibrous membranes as a function of (c) applied pressure and (d) shockwave duration. (*$p<0.05$, **$p<0.01$, the red dotted lines indicate the minimal amounts of drug release from non-piezo controls). On-demand (e) drug release and (f) remaining drug profile of poly(l-lysine)-Vivotag-645-loaded P(VDF-TrFE) nanofibrous membranes, where the membranes were stimulated by shockwaves at 3 bar/12 Hz for 2 mins every 2 days (insets: photoluminescence images of porcine skins).

4. Discussion

The development of controlled drug delivery systems has been extensively investigated to improve the therapeutic efficacy of conventional drug products. Especially, many studies have demonstrated the effective therapeutic performance of nanotechnology-based delivery systems[26-]

[29]. Despite the favorable surface-to-volume ratio of these nanomaterials, instability *in vivo* and inferior biocompatibility limited their use for *in vivo* applications[30, 31]. Furthermore, typical characteristics of passive drug release mechanisms from these systems do not allow for modifications in response to temporally changing therapeutic needs commonly required in chronic diseases. This has instigated many researchers to focus on developing stimuli-responsive polymers for precise control over the release. Unlike physiological change-responsive mechanisms, such as pH or temperature, external stimuli-responsiveness, including mechanical force or magnetic field, offer greater controllability over the drug release.

In this study, a novel stimuli-responsive drug delivery system that can be activated by mechanical stimulation was developed utilizing a piezoelectric nanofibrous membrane. The capability of piezoelectric material in generating electric potentials in response to mechanical perturbation enables the release of electrostatically adsorbed drugs, providing a new avenue as a controlled drug delivery vehicle. One of the major obstacles in utilizing piezoelectric material for drug delivery vehicles is that the material needs to be activated under physiologically safe mechanical loading. Despite the high piezoelectricity of ceramic-based materials, their biotoxicity or instability in aqueous conditions limits *in vivo* applications. In this regard, we have previously shown the advantage of utilizing electrospinning for a transformative piezoelectric enhancement of P(VDF-TrFE) polymer via nanoscale dimensional reduction and appropriate heat treatment[22], making the polymer sensitive to physiologically safe mechanical stimulus and ideal for developing a drug delivery system that is precisely controllable by the applied magnitude of mechanical stimulation.

Despite the change in the piezoelectric coefficient of the nanofibers with varying diameters, the zeta potential analysis revealed that the surface charge remains negative above pH 3 for all P(VDF-

TrFE) and PVDF samples. These isoelectric points were beyond the titrated concentrations of HCl during the measurement and irrelevant to the use of drug release in practical *in vivo* applications, preventing any uncontrolled diffusion-based release. Indeed, both of our repeated on-demand release tests *in vitro* and *ex vivo* showed no drug leaks during prolonged incubation periods. These zeta potential values agree closely with those reported in the literature for PVDF films and membranes[32-35], although the explanation for the persistent negative surface of PVDF remains ambiguous throughout literature[33]. Nevertheless, cationic molecules such as crystal violet and poly(l-lysine) used as model drugs in our study, readily adsorbed onto the negatively charged surface of P(VDF-TrFE) nanofibrous membranes. The selectivity of drug loading on P(VDF-TrFE) nanofibrous membranes was confirmed, where both anionic molecule, Eosin Y (Sigma), and hydrophobic molecule, Oil Red O (Sigma), were unable to be stably adsorbed onto P(VDF-TrFE) nanofibrous membranes (**Figure S4**).

The drug release from P(VDF-TrFE) nanofibers with various diameters was investigated to show the size-dependent or piezoelectric property-dependent effects on the drug release tunability. With decreasing nanofiber diameter, an increase in drug release was observed. With nanofibers below 100 nm, there was an exponential increase in drug release. This can be attributed to the transformative enhancement of piezoelectric properties when the nanofibers are synthesized well below the nanoscale (<100 nm), which induces both greater alignment in piezoelectric domains and materialization of flexoelectricity[22]. Furthermore, an insignificant amount of drug released from the non-piezoelectric control, heat-inactivated PVDF nanofibrous membrane shows that drug release is independent of direct mechanical stimulation. This is further affirmed with the similar zeta potentials of the samples, together with similarity in the material chemistry, enabling the development of a mechano-responsive platform based purely on piezoelectricity. Similar to how

other drug delivery platforms use pore size or material degradation rate to control the amount of drug released over time[36, 37], these results collectively demonstrate that the sensitivity of the piezoelectric fibers to a given mechanical stimulation can be tuned for specific therapeutic applications. For example, less sensitive piezoelectric fibers can be used for subcutaneously implanted drug delivery systems to avoid false activation by accidental impact while highly sensitive piezoelectric nanofibers are desired for the use in deep tissues to be activated with a physiologically safe magnitude of mechanical stimulation.

The high-performing 30 nm P(VDF-TrFE) fibers were utilized to investigate the effect of applied pressure on drug release. From 1 to 2.5 bar a linear trend is observed which we attribute to the initial linear compression of the PDMS-sample-PDMS *in vitro* construct. These forces may produce an electric potential close to, but not completely over the zero-zeta potential point. Thus, a small amount of dye is released at this range. The applied pressure from 3-5 bar begins to affect the compressive elastic region of PDMS. More specifically, as the shockwave is set to a fixed pressure acting on a compressible material (i.e., PDMS), the stress transfer to the PDMS, and subsequently to the P(VDF-TrFE) nanofibrous membrane, rises exponentially as a function of strain applied to the PDMS layer. As a result, the piezoelectric nanofibrous membrane undergoes full direct piezoelectric effect and responds proportionally to the exponentially increasing applied stress, as described by the equation:

$$D_i = d_{ikl}T_{kl} + \varepsilon_{ik}^{T}\phi_k,$$

where D is the electric displacement, d is the piezoelectric charge coefficient with units of m V^{-1} or C N^{-1}, and T is applied stress. The second term on the right-hand side of the equation goes to zero in cases where an external electric field is absent or otherwise contributes to the electric displacement in the presence of an electric field proportional to the dielectric constant of the

material at a constant stress value (T superscript). As a result of the piezoelectric effect, the nanofibrous membrane overcomes the potential barrier, and an exponential drug release is observed for pressures above 3 bar. Moreover, as the electrostatic attraction between the negatively charged fiber surface and the cationic drug is switched (zeta potential approaching and going towards positive values) the drug molecule is released and repelled from the fiber surface and diffuses towards the capturing film or hydrogel. This is similar to materials undergoing ferroelectric switching where switchable forces of attraction and repulsion on charged probes within the double layer formed depending on the state of polarization of the material[38]. Although the model drugs used here are cationic, we propose that the use of anionic-based molecules is possible with the proper pre-functionalization of the P(VDF-TrFE) nanofibrous membrane surface with a cationic linker, still working under the same principle.

Drug release as a function of shockwave dosage showed a positive linear trend, indicative of precise control over the release of adsorbed drug molecules. Compared to more traditional drug delivery systems based on degradation or diffusion release that typically shows multiphasic profiles with an initial burst release[36, 39, 40], the linear profile of drug release from the piezoelectric-based system allows for the precise administration of drug molecules regardless of implantation duration. Moreover, since the same sample was used to survey the release response from 1 to 5 bar, the ability of the nanofibrous membrane to maintain a consistent release rate independent of the previous release history is also attractive. Similarly, the repeated on-demand drug release tests both *in vitro* and *ex vivo* showed a similar amount of drug release, confirming the robust control of release rate.

The results from our hydrogel *in vitro* model and porcine skin *ex vivo* model strongly suggest the potential of utilizing the piezoelectric nanofibrous membrane as a mechano-responsive drug

carrier for *in vivo* applications. Extracorporeal shockwave system, employed as a mechanical stimulator in our study, has been implemented therapeutically in reducing pain caused by chronic pelvic pain syndrome[41], calcifying tendonitis[41], fragmenting kidney stones[42], or triggering anti-inflammatory actions associated with many inflammatory diseases[43]. It was observed that the shockwave did not alter the structure of the porcine skin after actuation. Considering effective shockwave propagation through biological tissues/organs, this mode of activating the piezoelectric nanofibers is not limited to extreme discomfort needed to achieve release, e.g. in temperature-responsive systems, or attenuation of stimulus, e.g., light-responsive systems. The *ex vivo* results are an encouraging prediction of the *in vivo* behavior of drug-loaded piezoelectric nanofibers under mechanical actuation. A recent study demonstrated the feasibility of utilizing piezoelectric P(VDF-TrFE) for controlled drug delivery applications by the addition of magnetic material as a piezoelectric activator under the applied magnetic fields[44]. In addition to its complex synthesizing process limiting mass-producibility, the cost and limited availability of the activation system for such a strategy (i.e., MRI) is a strong impetus for employing our alternative approach, where a widely available hand-held shockwave system can activate the piezoelectric material for on-demand drug release. Altogether, our results suggest diverse ways of controlling drug release from this stimulus-responsive piezoelectric system: the dosage and magnitude of shockwaves, or different levels of piezoelectric sensitivity by controlling the fiber diameter.

5. Conclusions

In summary, we have developed a mechano-responsive drug delivery system based on a piezoelectric nanofibrous membrane, where surface potential changes by exogenous mechanical actuation trigger the release of drug molecules electrostatically adsorbed on the polymer. We

demonstrated that drug release kinetics can be controlled by the modulation of polymer piezoelectric properties or the magnitude/dosage of mechanical stimulation. 3D *in vitro* and *ex vivo* models were utilized to verify the controllability of drug release in a physiologically relevant environment. Overall, we demonstrated the novel utility of piezoelectric electrospun nanofibers for mechano-responsive controlled drug release and its potential for *in vivo* applications in a facile manner.

Supporting Information

Figure S1. Molecular structures of crystal violet and poly(l-lysine), and spectral properties of crystal violet and Vivotag-645.

Figure S2. Calibration curve of a cationic model drug (crystal violet) concentration for 2D *in vitro* study.

Figure S3. Calibration curve of a cationic model drug (crystal violet) concentration for 3D *in vitro* study.

Figure S4. Selective loading of EosinY and Oil Red O onto P(VDF-TrFE) membranes with 30 nm fiber diameter.

Corresponding Author

Jin Nam, Ph.D., Department of Bioengineering, University of California, Riverside, Riverside, CA 92521, E-mail: jnam@engr.ucr.edu, Tel: 951-827-2064

Author Contributions

The manuscript was written through the contributions of all authors. All authors have given approval to the final version of the manuscript. ‡These authors contributed equally.

ABBREVIATIONS

P(VDF-TrFE), poly(vinylidene fluoride-trifluroethylene); PZT, zirconate titanate; ZnO, zinc oxide; $BaTiO_3$, barium titanate; DMF, N,N-dimethylformamide; THF, tetrahydrofuran; PF, pyridinium formate; SEM, scanning electron microscope; PPLN, poled lithium niobite; PFM, piezoresponse force microscopy; PLL, poly(l-lysine); GelMA, gelatin methacrylate; ANOVA, analysis of variance.

REFERENCES

1.   Coelho, J. F.; Ferreira, P. C.; Alves, P.; Cordeiro, R.; Fonseca, A. C.; Gois, J. R.; Gil, M. H., Drug delivery systems: Advanced technologies potentially applicable in personalized treatments. *EPMA J* **2010,** *1* (1), 164-209.

2.   Senapati, S.; Mahanta, A. K.; Kumar, S.; Maiti, P., Controlled drug delivery vehicles for cancer treatment and their performance. *Signal Transduct Target Ther* **2018,** *3*, 7.

3.   Singh, R.; Lillard, J. W., Jr., Nanoparticle-based targeted drug delivery. *Exp Mol Pathol* **2009,** *86* (3), 215-23.

4.   Galvin, P.; Thompson, D.; Ryan, K. B.; McCarthy, A.; Moore, A. C.; Burke, C. S.; Dyson, M.; Maccraith, B. D.; Gun'ko, Y. K.; Byrne, M. T.; Volkov, Y.; Keely, C.; Keehan, E.; Howe, M.; Duffy, C.; MacLoughlin, R., Nanoparticle-based drug delivery: case studies for cancer and cardiovascular applications. *Cell Mol Life Sci* **2012,** *69* (3), 389-404.

5.   Gao, W.; Chan, J. M.; Farokhzad, O. C., pH-Responsive Nanoparticles for Drug Delivery. *Molecular Pharmaceutics* **2010,** *7* (6), 1913-1920.

6.   Zheng, C.; Wang, Y.; Phua, S. Z. F.; Lim, W. Q.; Zhao, Y., ZnO–DOX@ZIF-8 Core–Shell Nanoparticles for pH-Responsive Drug Delivery. *ACS Biomaterials Science & Engineering* **2017,** *3* (10), 2223-2229.

7.   Zheng, Y.; Wang, L.; Lu, L.; Wang, Q.; Benicewicz, B. C., pH and Thermal Dual-Responsive Nanoparticles for Controlled Drug Delivery with High Loading Content. *ACS Omega* **2017,** *2* (7), 3399-3405.

8.   Huu, V. A.; Luo, J.; Zhu, J.; Zhu, J.; Patel, S.; Boone, A.; Mahmoud, E.; McFearin, C.; Olejniczak, J.; de Gracia Lux, C.; Lux, J.; Fomina, N.; Huynh, M.; Zhang, K.; Almutairi, A., Light-responsive nanoparticle depot to control release of a small molecule angiogenesis inhibitor in the posterior segment of the eye. *J Control Release* **2015,** *200*, 71-7.

9.   Imanifard, S.; Zarrabi, A.; Zarepour, A.; Jafari, M.; Khosravi, A.; Razmjou, A., Nanoengineered Thermoresponsive Magnetic Nanoparticles for Drug Controlled Release. *Macromolecular Chemistry and Physics* **2017,** *218* (23), 1700350.

10.   Kong, S. D.; Sartor, M.; Hu, C. M.; Zhang, W.; Zhang, L.; Jin, S., Magnetic field activated lipid-polymer hybrid nanoparticles for stimuli-responsive drug release. *Acta Biomater* **2013,** *9* (3), 5447-52.

11.   Papa, A. L.; Korin, N.; Kanapathipillai, M.; Mammoto, A.; Mammoto, T.; Jiang, A.; Mannix, R.; Uzun, O.; Johnson, C.; Bhatta, D.; Cuneo, G.; Ingber, D. E., Ultrasound-sensitive nanoparticle aggregates for targeted drug delivery. *Biomaterials* **2017,** *139*, 187-194.

12.   Wang, Y.; Deng, Y.; Luo, H.; Zhu, A.; Ke, H.; Yang, H.; Chen, H., Light-Responsive Nanoparticles for Highly Efficient Cytoplasmic Delivery of Anticancer Agents. *ACS Nano* **2017,** *11* (12), 12134-12144.

13.   Zhou, J.; Pishko, M. V.; Lutkenhaus, J. L., Thermoresponsive layer-by-layer assemblies for nanoparticle-based drug delivery. *Langmuir* **2014,** *30* (20), 5903-10.

14.   Weaver, C. L.; LaRosa, J. M.; Luo, X.; Cui, X. T., Electrically controlled drug delivery from graphene oxide nanocomposite films. *ACS Nano* **2014,** *8* (2), 1834-43.

15.   Chao-Nan, X.; Akiyama, M.; Nonaka, K.; Watanabe, T., Electrical power generation characteristics of PZT piezoelectric ceramics. *IEEE Transactions on Ultrasonics, Ferroelectrics, and Frequency Control* **1998,** *45* (4), 1065-1070.

16.   Karaki, T.; Yan, K.; Miyamoto, T.; Adachi, M., Lead-Free Piezoelectric Ceramics with Large Dielectric and Piezoelectric Constants Manufactured from BaTiO3Nano-Powder. *Japanese Journal of Applied Physics* **2007,** *46* (No. 4), L97-L98.

17.   Jacob, J.; More, N.; Kalia, K.; Kapusetti, G., Piezoelectric smart biomaterials for bone and cartilage tissue engineering. *Inflamm Regen* **2018,** *38*, 2.

18.   Rajabi, A. H.; Jaffe, M.; Arinzeh, T. L., Piezoelectric materials for tissue regeneration: A review. *Acta Biomater* **2015,** *24*, 12-23.

19.   Valentini, R. F.; Sabatini, A. M.; Dario, P.; Aebischer, P., Polymer electret guidance channels enhance peripheral nerve regeneration in mice. *Brain Res* **1989,** *480* (1-2), 300-4.

20.   Laroche, G.; Marois, Y.; Guidoin, R.; King, M. W.; Martin, L.; How, T.; Douville, Y., Polyvinylidene fluoride (PVDF) as a biomaterial: from polymeric raw material to monofilament vascular suture. *J Biomed Mater Res* **1995,** *29* (12), 1525-36.

21.   Wells, R. G., Tissue mechanics and fibrosis. *Biochim Biophys Acta* **2013,** *1832* (7), 884-90.

22.   Ico, G.; Myung, A.; Kim, B. S.; Myung, N. V.; Nam, J., Transformative piezoelectric enhancement of P(VDF-TrFE) synergistically driven by nanoscale dimensional reduction and thermal treatment. *Nanoscale* **2018,** *10* (6), 2894-2901.

23. Steinmann, W.; Walter, S.; Seide, G.; Gries, T.; Roth, G.; Schubnell, M. Structure, Properties, And Phase Transitions Of Melt-Spun Poly(Vinylidene Fluoride) Fibers. Journal of Applied Polymer Science 2010, 120, 21-35.

24. Nichol, J. W.; Koshy, S. T.; Bae, H.; Hwang, C. M.; Yamanlar, S.; Khademhosseini, A., Cell-laden microengineered gelatin methacrylate hydrogels. *Biomaterials* **2010,** *31* (21), 5536-44.

25. Ico, G.; Showalter, A.; Bosze, W.; Gott, S. C.; Kim, B. S.; Rao, M. P.; Myung, N. V.; Nam, J., Size-dependent piezoelectric and mechanical properties of electrospun P(VDF-TrFE) nanofibers for enhanced energy harvesting. *Journal of Materials Chemistry A* **2016,** *4* (6), 2293-2304.

26. Fox, M. E.; Guillaudeu, S.; Frechet, J. M.; Jerger, K.; Macaraeg, N.; Szoka, F. C., Synthesis and *in vivo* antitumor efficacy of PEGylated poly(l-lysine) dendrimer-camptothecin conjugates. *Mol Pharm* **2009,** *6* (5), 1562-72.

27. Lee, G. Y.; Qian, W. P.; Wang, L.; Wang, Y. A.; Staley, C. A.; Satpathy, M.; Nie, S.; Mao, H.; Yang, L., Theranostic nanoparticles with controlled release of gemcitabine for targeted therapy and MRI of pancreatic cancer. *ACS Nano* **2013,** *7* (3), 2078-89.

28. Mikhaylov, G.; Mikac, U.; Magaeva, A. A.; Itin, V. I.; Naiden, E. P.; Psakhye, I.; Babes, L.; Reinheckel, T.; Peters, C.; Zeiser, R.; Bogyo, M.; Turk, V.; Psakhye, S. G.; Turk, B.; Vasiljeva, O., Ferri-liposomes as an MRI-visible drug-delivery system for targeting tumours and their microenvironment. *Nat Nanotechnol* **2011,** *6* (9), 594-602.

29.   Rosenholm, J. M.; Peuhu, E.; Bate-Eya, L. T.; Eriksson, J. E.; Sahlgren, C.; Linden, M., Cancer-cell-specific induction of apoptosis using mesoporous silica nanoparticles as drug-delivery vectors. *Small* **2010,** *6* (11), 1234-41.

30.   Ghosn, Y.; Kamareddine, M. H.; Tawk, A.; Elia, C.; El Mahmoud, A.; Terro, K.; El Harake, N.; El-Baba, B.; Makdessi, J.; Farhat, S., Inorganic Nanoparticles as Drug Delivery Systems and Their Potential Role in the Treatment of Chronic Myelogenous Leukaemia. *Technol Cancer Res Treat* **2019,** *18*, 1533033819853241.

31.   Singh, A. P.; Biswas, A.; Shukla, A.; Maiti, P., Targeted therapy in chronic diseases using nanomaterial-based drug delivery vehicles. *Signal Transduct Target Ther* **2019,** *4*, 33.

32.   Breite, D.; Went, M.; Prager, A.; Schulze, A., Tailoring Membrane Surface Charges: A Novel Study on Electrostatic Interactions during Membrane Fouling. *Polymers* **2015,** *7* (10), 2017-2030.

33.   Chen, Y.; Tian, M.; Li, X.; Wang, Y.; An, A. K.; Fang, J.; He, T., Anti-wetting behavior of negatively charged superhydrophobic PVDF membranes in direct contact membrane distillation of emulsified wastewaters. *Journal of Membrane Science* **2017,** *535*, 230-238.

34.   Guo, J.; Farid, M. U.; Lee, E.-J.; Yan, D. Y.-S.; Jeong, S.; Kyoungjin An, A., Fouling behavior of negatively charged PVDF membrane in membrane distillation for removal of antibiotics from wastewater. *Journal of Membrane Science* **2018,** *551*, 12-19.

35.   Schulze, A.; Went, M.; Prager, A., Membrane Functionalization with Hyperbranched Polymers. *Materials (Basel)* **2016,** *9* (8).

36. Kumari, A.; Yadav, S. K.; Yadav, S. C., Biodegradable polymeric nanoparticles based drug delivery systems. *Colloids Surf B Biointerfaces* **2010,** *75* (1), 1-18.

37. Wang, Y.; Zhao, Q.; Han, N.; Bai, L.; Li, J.; Liu, J.; Che, E.; Hu, L.; Zhang, Q.; Jiang, T.; Wang, S., Mesoporous silica nanoparticles in drug delivery and biomedical applications. *Nanomedicine* **2015,** *11* (2), 313-27.

38. Ferris, R. J.; Lin, S.; Therezien, M.; Yellen, B. B.; Zauscher, S., Electric double layer formed by polarized ferroelectric thin films. *ACS Appl Mater Interfaces* **2013,** *5* (7), 2610-7.

39. Huang, J.; Shu, Q.; Wang, L.; Wu, H.; Wang, A. Y.; Mao, H., Layer-by-layer assembled milk protein coated magnetic nanoparticle enabled oral drug delivery with high stability in stomach and enzyme-responsive release in small intestine. *Biomaterials* **2015,** *39*, 105-13.

40. Kamaly, N.; Yameen, B.; Wu, J.; Farokhzad, O. C., Degradable Controlled-Release Polymers and Polymeric Nanoparticles: Mechanisms of Controlling Drug Release. *Chem Rev* **2016,** *116* (4), 2602-63.

41. Zimmermann, R.; Cumpanas, A.; Miclea, F.; Janetschek, G., Extracorporeal shock wave therapy for the treatment of chronic pelvic pain syndrome in males: a randomised, double-blind, placebo-controlled study. *Eur Urol* **2009,** *56* (3), 418-24.

42. Osman, M. M.; Alfano, Y.; Kamp, S.; Haecker, A.; Alken, P.; Michel, M. S.; Knoll, T., 5-year-follow-up of patients with clinically insignificant residual fragments after extracorporeal shockwave lithotripsy. *Eur Urol* **2005,** *47* (6), 860-4.

43.   Mariotto, S.; de Prati, A. C.; Cavalieri, E.; Amelio, E.; Marlinghaus, E.; Suzuki, H., Extracorporeal shock wave therapy in inflammatory diseases: molecular mechanism that triggers anti-inflammatory action. Curr Med Chem 2009, 16 (19), 2366-72.

44.   Mushtaq, F.; Torlakcik, H.; Hoop, M.; Jang, B.; Carlson, F.; Grunow, T.; Läubli, N.; Ferreira, A.; Chen, X.; Nelson, B. et al. Motile Piezoelectric Nanoeels For Targeted Drug Delivery. Advanced Functional Materials 2019, 29, 1808135.

For Table of Contents Only